3-26-2008

Storage and Retrieval of Multimode Transverse Images in Hot Atomic Rubidium Vapor

Praveen K. Vudyasetu
University of Rochester

Ryan M. Camacho
University of Rochester

John C. Howell
Chapman University, johhowell@chapman.edu

Recommended Citation

P. K. Vudyasetu, R. M. Camacho, and J. C. Howell,*Storage and Retrieval of Multimode Transverse Images in Hot Atomic Rubidium Vapor*, Phys. Rev. Lett. **100**(12), 123903. https://doi.org/10.1103/PhysRevLett.100.123903

Storage and Retrieval of Multimode Transverse Images in Hot Atomic Rubidium Vapor

Storage and Retrieval of Multimode Transverse Images in Hot Atomic Rubidium Vapor

Praveen K. Vudyasetu, Ryan M. Camacho, and John C. Howell

Department of Physics and Astronomy, University of Rochester, Rochester, New York 14627, USA

(Received 5 December 2007; published 26 March 2008)

We report on the experimental realization of the storage of images in a hot vapor of Rubidium atoms. The images are stored in and retrieved from the long-lived ground state atomic coherences. We show that an image impressed onto a 500 ns pulse can be stored and retrieved up to 30 μs later. The image storage is made robust to diffusion by storing the Fourier transform of the image.

DOI: 10.1103/PhysRevLett.100.123903 PACS numbers: 42.30.−d, 42.50.Gy, 42.50.Md, 42.70.Ln

''Stopped light'' usually refers to the interconversion of electromagnetic fields into long-lived atomic coherences. It allows for the recording of coherent signals for later retrieval even at very low light levels. The initial work by Liu *et al.* [1] and Phillips *et al.* [2] stimulated additional research with a recent demonstration of storage times in excess of 1 s [3]. Stopped light may be useful for applications in remote sensing, image processing, and quantum information.

Typically, the pulses used in stopped light experiments are several kilometers long in free space. However, the stopped light medium usually ranges from a few tens of microns up to several centimeters, so slow light is first used to spatially compress the optical pulses inside the medium. Slow light is achieved when a steep linear dispersion can be obtained in a medium, leading to a large group index $n_g = n + \omega \frac{\partial n}{\partial \omega}$ and small group velocity $v_g = c/n_g$, where n is the phase index and ω is the angular frequency. Slow group velocities have been achieved in a variety of media, including atomic vapors [1,4–9] and solids [10–16].

Recently there has been some interest in extending the ideas of single transverse mode slow and stopped light to multiple transverse modes where the atomic medium delays and stores the spatial profiles of the stored pulses [17–21]. One of the difficulties of using hot vapors as the storage medium for stopped light experiments is the diffusion of atoms during storage period. Recently, Pugatch *et al.* [19] showed that an optical vortex with a phase singularity in the transverse spatial profile can be stored in an atomic medium despite strong diffusion. Subsequently, there has been some theoretical work done to make image storage in hot vapors robust to diffusion [20].

In this Letter, we demonstrate the storage and retrieval of a transverse image in a hot atomic vapor using a combination of electromagnetically induced transparency (EIT)[22] and four-wave mixing (FWM) techniques. We overcome the adverse effects of diffusion by storing the Fourier transform of the image in the stopped light medium rather than the image itself. While the optical phase in the object plane is constant, the phase in the Fourier plane varies in such a way that atoms with opposite phase destructively interfere during diffusion [20]. This is similar to the storage of the Laguerre-Gauss beams [19] under diffusion where atoms on opposite sides of the phase singularity have relative phases of π and destructively interfere.

A schematic of the experimental setup is shown in Fig. 1(a). A 12.5 cm long Rb vapor cell with natural isotopic abundance containing 20 torr neon buffer gas is placed in a magnetically shielded oven and heated to approximately 180 °C, yielding a number density of approximately 10^{13} atoms/cm^3. A $4f$ imaging system is used to image the object onto the camera as well as place the Fourier plane at the cell. It consists of two lenses, L_1 and L_2, each of focal length $f = 500$ mm separated by a distance $2f$. The object is placed at the front focal plane of L_1 and the image is obtained at the back focal plane of L_2. The vapor cell is placed at the back focal plane of L_1 (the Fourier plane). The diameter of the cell is 1 cm and the transverse diameter of the signal beam is chosen such that the profile of Fourier image fits in the cell. The pump beam is orthogonally polarized to the signal to filter out the pump. In addition to polarization filtering, we also performed a temporal filtering correlation measurement using a 100 MHz detector (3 dB roll off). A 25 μm slit is placed in the focal plane and a bucket detector is placed behind the slit. The position of the slit is scanned in the image plane and the temporal intensity profile of the retrieved light pulse hitting the bucket detector is recorded on a 1.5 GHz oscilloscope.

Our slow light scheme is based on a combination of EIT and FWM in a Λ system which consists of two lower energy levels coupled to a common higher energy level of the atom by two electromagnetic fields. The relevant energy levels of ^{85}Rb are shown in Fig. 1(b). To obtain a highly transparent region which also exhibits steep dispersion, the pump and signal lasers are detuned several hundred MHz from the zero velocity class in a Doppler broadened vapor. The signal experiences both FWM gain and EIT when its frequency is tuned to the two-photon Raman resonance. As a note, optical alignment, buffer gas pressures, laser detunings, etc., all affect the transmission and dispersion. The rapid change in the transmission profile near Raman resonance leads to steep dispersion and

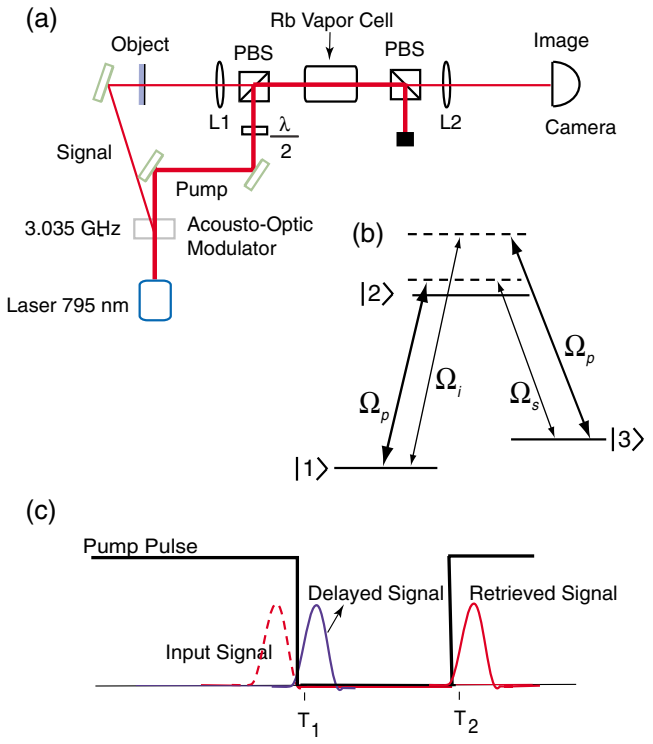

FIG. 1 (color online). (a) An external cavity diode laser followed by an amplifier is the source for pump beam. The signal is generated by frequency shifting part of the pump by 3.035 Ghz using an acousto-optic modulator. The $1/e^2$ beam diameter of the pump is approximately 4 mm and that of signal approximately 1 mm at the object plane. The powers of pump and signal beams are approximately 12 mW and 300 μW respectively. The pump and signal beams are orthogonally polarized and are combined using a polarizing beam splitter (PBS) before the cell. The pump is filtered from the signal using another PBS after the cell. The object, lenses L_1 and L_2, and the camera form a $4f$ imaging system. (b) We use the D_1 transitions of ^{85}Rb to create a Λ configuration. The pump is detuned by 700 MHz to the blue of the optical transition connecting the $F = 2$ ground state to the $F' = (2, 3)$ excited states, and the signal is set 3.035 GHz (the ground state hyperfine splitting) to the red of the pump. (c) Representation of the synchronized timing of signal (dashed red), delayed signal (blue) and pump (black) beams. Once a signal pulse is inside the medium, the pump beam is turned off at time T_1, storing the image. The pump beam is then turned back on at time T_2, retrieving the stored image pulse (solid red).

slow group velocity. Once the signal has been compressed inside the cell, we turn off the pump, storing the image. The transverse spatial profile of the signal is mapped onto the long-lived ground state coherence of the ^{85}Rb atoms. The signal is retrieved by turning on the pump at a later time. The timing of the pulses is illustrated in Fig. 1(c). The intensity profile of the signal at the object plane and its Fourier transform at the vapor cell are shown in Fig. 2. The retrieved signal intensity falls off exponentially with storage time due to diffusion and decoherence.

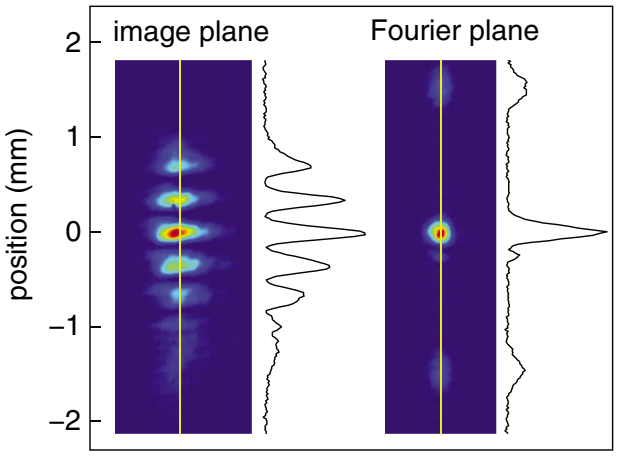

FIG. 2 (color online). CCD camera capture of the signal intensity profile at the object plane and at the vapor cell (Fourier plane).

Figure 3 shows the input image (a), as well as the retrieved (b) and calculated (c) image profiles for several storage times. The theory plots are generated by using Eq. (4) to propagate the measured input image shown in Fig. 3(a). The object used is an amplitude mask containing a 5 bar test pattern. We note that the image contrast remains high even for the longer storage times, even though the wings of the image decay faster than the central part, as predicted by diffusion theory. The physical mechanism responsible for preserving the image can be understood in terms of the phase distribution of the stored optical wavefront and the diffusion of the atoms (shown graphically in Fig. 4). Each atom in the field acquires the local coherence set by the signal and pump fields. As the atoms diffuse in the Fourier plane, atoms of opposite phase tend to destructively interfere preserving the high contrast. This is similar to the topological stability of stored Laguerre-Gauss beams as demonstrated by Pugatch *et al.* and in good agreement with the theoretical predictions by Zhao *et al.* We adopt the diffusion model of Pugatch *et al.* to simulate image diffusion in the Fourier plane. We first determine the Fourier transform of the field in the back focal plane of L_1. Let E_o be the field at the object plane which is also the front focal plane of a spherical lens of focal length f. At the back focal plane of the lens, the field E_f is given by the Fourier transform of the field in the object plane:

$$E_f = F(E_o) = \frac{1}{\sqrt{\lambda f}} \int_{-\infty}^{\infty} E_o \exp\left(-i\frac{2\pi}{\lambda f}\xi u\right) d\xi, \quad (1)$$

where ξ and u are the coordinates of object plane and Fourier transform plane, respectively. The ground state atomic coherence at the time of storage is given by $\rho_{13} = g\Omega_s$, where g is the nonlinear coupling coefficient and Ω_s is the Rabi frequency of the signal field. The time evolution of the atomic coherence is given by

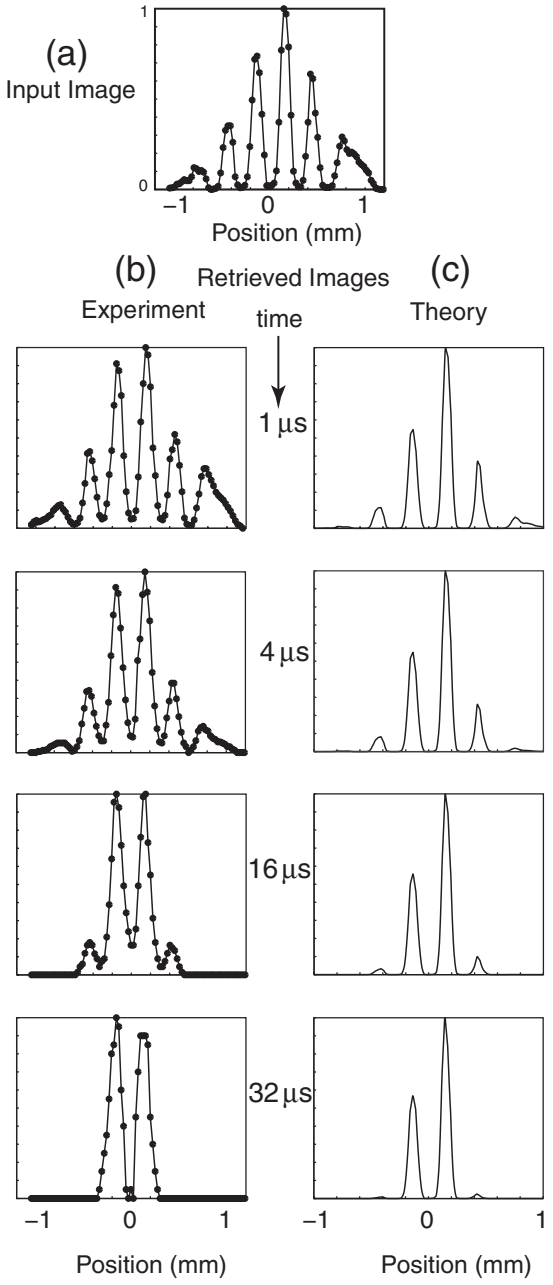

FIG. 3. Input signal profile (a) and the time evolution of measured (b) and calculated (c) transverse images. The theory plots are generated using Eq. (4) with a diffusion coefficient of 10 cm^2/s).

$$\frac{\partial \rho_{13}(u,t)}{\partial t} = D\frac{\partial^2 \rho_{13}}{\partial u^2} - \frac{\rho_{13}}{T_c} \tag{2}$$

where T_c is ground state decoherence time of the coherence ρ_{13}, and D is the diffusion coefficient of the atoms. Assuming a constant pump intensity along the transverse dimension of the cell, the only spatial dependence of the ground state coherence comes from the signal field amplitude.

Figure 4 shows the evolution of the ground state coherence under the conditions of decoherence and diffusion. The inset of the figure shows a section of plot containing zero crossover points. We see that the zeros of ρ_{13} are unchanged, though the amplitude on either side of zero crossovers decreases with time. As the atoms with positive and negative phases have equal probability of reaching the zero crossover point, the retrieved fields from such atoms at those points tend to destructively interfere, maintaining a zero in the field amplitude. At other points, the same interference process results in a decrease in amplitude while maintaining the field profile.

The field at the image plane, E_i, is recovered by inserting Eq. (1) into the diffusion equation [Eq. (2)] and taking another Fourier transform, which upon integration gives

$$\frac{\partial}{\partial t}E_i(x,t) = -\left(\frac{1}{T_d} + \frac{1}{T_c}\right)E_i(x,t), \tag{3}$$

with a solution given by

$$E_i(x,t) = E_i(x,0)\exp\left[-t\left(\frac{1}{T_d} + \frac{1}{T_c}\right)\right], \tag{4}$$

where $T_d = \frac{\lambda^2 f^2}{(2\pi)^2 D x^2}$ is the diffusion time constant and x is the coordinate in the image plane.

We note that by integrating over the spatial coordinate u at the cell from negative infinity to positive infinity we have not accounted for the finite numerical aperture of the $4f$ imaging system. The size of the numerical aperture in our system is set by the size of the pump beam at the cell, which has a $1/e^2$ intensity diameter of approximately

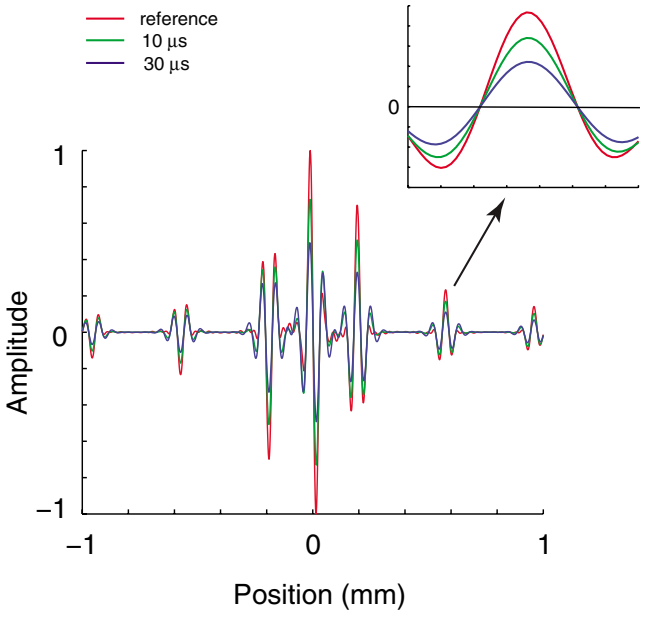

FIG. 4 (color online). Theoretical time evolution of stored ground state coherence of Rb atoms. The inset shows a close-up of the time evolution near zero crossover points of electric field amplitude.

4 mm. Since this is larger than the spatial extent of all relevant features in the Fourier transformed image (see Fig. 2), this approximation is valid. In addition, we have assumed that all modes of spatial diffusion for the prepared atoms remain within the pump beam diameter, so that higher order modes which exit from and then return to the pump beam during storage do not cause interference [23]. Since the diffusion length for the longest storage time is given by $\sqrt{Dt} \approx 170\ \mu$m, and the closest relevant feature in the Fourier transform of the image is farther than 500 μm from the edge of the pump beam, this is also a reasonable assumption. As a note, we also performed numerical integration over the relevant finite dimensions of our experiment which produced negligible errors.

There are two features worth noting in Eq. (4). First, each spatial point in the image decays exponentially in time, with a time constant given by $1/T_d + 1/T_c$. This means that dark areas of the image remain dark for appreciable times compared to the temporal pulse length. Second, since T_d falls off like $1/x^2$, the central portion of the image has maximum storage time. We can increase the diffusion time T_d by making the image smaller or making the focal length of the imaging lens larger. In either case, the Fourier transformed spatial profile at the vapor cell would be larger, requiring a correspondingly larger pump beam diameter and vapor cell.

In summary, we have slowed and stored an arbitrary transverse image in a hot atomic vapor, and shown that the retrieved image is robust to atomic diffusion. This remarkable feature allows the coherent storage of spatial information even in Doppler broadened media with large diffusion constants.

We gratefully acknowledge support from DARPA DSO Slow Light, the DOD MURI for Quantum Imaging and the National Science Foundation.

Note added in proof.—As a note, we have recently become aware of image storage in a similar system [24].

[1] C. Liu, Z. Dutton, C. H. Behroozi, and L. V. Hau, Nature (London) **409**, 490 (2001).
[2] D. F. Phillips, A. Fleischhauer, A. Mair, and R. L. Walsworth, Phys. Rev. Lett. **86**, 783 (2001).
[3] J. J. Longdell, E. Fraval, M. J. Sellars, and N. B. Manson, Phys. Rev. Lett. **95**, 063601 (2005).
[4] S. E. Harris, J. E. Field, and A. Kasapi, Phys. Rev. A **46**, R29 (1992).
[5] A. Kasapi, M. Jain, G. Y. Yin, and S. E. Harris, Phys. Rev. Lett. **74**, 2447 (1995).
[6] D. Budker, D. F. Kimball, S. M. Rochester, and V. V. Yashchuk, Phys. Rev. Lett. **83**, 1767 (1999).
[7] L. V. Hau, S. E. Harris, Z. Dutton, and C. H. Behroozi, Nature (London) **397**, 594 (1999).
[8] W. G. Yang, D. B. Conkey, B. Wu, D. L. Yin, A. R. Hawkins, and H. Schmidt, Nat. Photon. **1**, 331 (2007).
[9] V. Boyer, C. McCormick, E. Arimondo, and P. D. Lett, arXiv:quant-ph/0703173.
[10] M. S. Bigelow, N. N. Lepeshkin, and R. W. Boyd, Phys. Rev. Lett. **90**, 113903 (2003).
[11] M. S. Bigelow, N. N. Lepeshkin, and R. W. Boyd, Science **301**, 200 (2003).
[12] J. B. Khurgin, J. Opt. Soc. Am. B **22**, 1062 (2005).
[13] G. M. Gehring, A. Schweinsberg, C. Barsi, N. Kostinski, and R. W. Boyd, Science **312**, 895 (2006).
[14] Z. M. Zhu and D. J. Gauthier, Opt. Express **14**, 7238 (2006).
[15] Y. Okawachi, M. A. Foster, J. E. Sharping, A. L. Gaeta, Q. F. Xu, and M. Lipson, Opt. Express **14**, 2317 (2006).
[16] E. Shumakher, N. Orbach, A. Nevet, D. Dahan, and G. Eisenstein, Opt. Express **14**, 5877 (2006).
[17] M. Jain, A. J. Merriam, A. Kasapi, G. Y. Yin, and S. E. Harris, Phys. Rev. Lett. **75**, 4385 (1995).
[18] R. M. Camacho, C. J. Broadbent, I. Ali-Khan, and J. C. Howell, Phys. Rev. Lett. **98**, 043902 (2007).
[19] R. Pugatch, M. Shuker, O. Firstenberg, A. Ron, and N. Davidson, Phys. Rev. Lett. **98**, 203601 (2007).
[20] L. Zhao, T. Wang, Y. Xiao, and S. F. Yelin, arXiv:0710.4144v1.
[21] M. Shuker, O. Firstenberg, R. Pugatch, A. Ben-Kish, A. Ron, and N. Davidson, Phys. Rev. A **76**, 023813 (2007).
[22] S. E. Harris, J. E. Field, and A. Imamoglu, Phys. Rev. Lett. **64**, 1107 (1990).
[23] Y. Xiao, I. Novikova, D. F. Phillips, and R. L. Walsworth, Phys. Rev. Lett. **96**, 043601 (2006).
[24] M. Shuker, O. Firstenberg, R. Pugatch, A. Ron, and N. Davidson, arXiv:0707.3707v1.